A Fast Method for Estimating Voxel Bone Volume Fractions from In Vivo High-Resolution MR Images

Scott Nyshin Hwang[1], Felix W. Wehrli[1]

[1]Laboratory for Structural NMR Imaging, University of Pennsylvania Medical Center, Department of Radiology, Philadelphia, PA USA;

Introduction

MR microimaging is uniquely suited for analyzing trabecular architecture (1-4). Since limited SNR precludes full resolution of trabeculae, binary segmentation, which assumes every voxel may be classified as containing one material phase only, discards potentially useful information. Previous work (5) described a method for obtaining maps of voxel bone volume fraction (BVF) by iterative deconvolution of the voxel intensity histogram. A drawback is the long computation time inherent to most iterative methods. A new method, referred to as "fast BVF mapping," is described and illustrated with *in vivo* MR images of the distal radius. The method's accuracy was evaluated with test images derived from micro-CT images of radius specimens.

Methods

Since bone appears with background intensity, marrow volume fraction may be computed as voxel intensity (I) divided by I_{marrow}, an estimate of the intensity of a voxel that contains marrow only. BVF would then be obtained as:

$$BVF[\mathbf{r}] = 1 - I[\mathbf{r}] / I_{marrow}[\mathbf{r}] \quad [1]$$

where $\mathbf{r}$ is the spatial location (x, y, z) of a voxel. BVF is obtained from Eq 1 after local marrow intensities are determined.

The method is illustrated with a typical *in vivo* 3D FLASE (fast large-angle spin-echo) (6, 7) image of the distal radius (Fig 1A, 137x137x350 micron^3 voxel size, 32 slices). The first step involves obtaining local classification thresholds for binary segmentation as local averages of voxels along the bone/marrow boundary, detected by morphologic edge enhancement. After binarization, noise voxels (i.e., incorrectly classified voxels) are reclassified using adjacency and connectivity criteria (Fig 1B). Voxels incorrectly classified as marrow are most likely those on the boundary of a trabecula and thus contain only a small fraction of bone. The algorithm attempts to select these voxels by reclassifying any marrow voxel, which has at least one bone-containing voxel among its 4 nearest neighbors, as bone (Fig 1C). Local marrow intensities are computed by locally averaging the unprocessed intensities of voxels, which are classified as marrow. To generate the BVF map (Fig 1D), the marrow voxels are assigned BVF=0 and the BVF of each bone voxel is computed from Eq 1.

Images for quantitatively evaluating fast BVF mapping were generated from three 3D micro-CT images of human radius specimens (22x22x22 micron^3 voxel size) (Fig 2A). "Gold standard" images were obtained by resampling to yield images with a voxel size of 132x132x352 micron^3, matching *in vivo* resolution. Test images (Fig 2B) were then created by adding Rician noise (8) to simulate an SNR of 10 as is typically obtained *in vivo* (7). Accuracy of fast BVF mapping was assessed by comparing average BVF and network length in each slice as determined from the gold standard images and from BVF maps derived from the test images.

Results and Discussion

Individual longitudinal and transverse trabeculae are evident in the 3D projection of the entire 3D BVF map of the *in vivo* radius image (Fig 1E). Fast BVF mapping of the entire 3D data set required less than 4 minutes on a 500MHz G3 PowerBook (Apple Computer). In addition to being noninvasive, MRI allows for structural analysis over a much larger volume than histomorphometry of bone biopsies.

The BVF maps (Fig 2C) were in excellent agreement with those of the gold standard images. BVF as well as structural parameters that depend on connectivity may be determined from the BVF map. In contrast, direct binary segmentation of the test image resulted in disconnected trabeculae when a classification threshold was chosen that yielded the correct slice BVF (Fig 2D). Lowering the threshold would better maintain connectivity but only at the expense of inflating BVF and becoming more sensitive to noise. The results of the quantitative evaluation are given in Fig 3, which show excellent agreement between the gold standard and the BVF map for both slice BVF (R^2=0.99, n=54) and slice network length (L) (R^2=0.91).

Conclusions

BVF maps generated from images obtained in the limited spatial resolution regime of *in vivo* micro-MRI have been demonstrated to yield correct BVF and network length, in contrast to binary segmentation. The speed and accuracy of the algorithm may help realize the potential of micro-MRI as a means of performing *in vivo* virtual bone biopsy for the purpose of assessing fracture risk and for monitoring the efficacy of therapy in osteopenic patients.

Acknowledgements

The authors are indebted to Dr. Laib and Prof. Peter Rüegsegger at the University and ETH Zurich for acquiring the micro-CT images. This work was supported by NIH Grant RO1 41443.

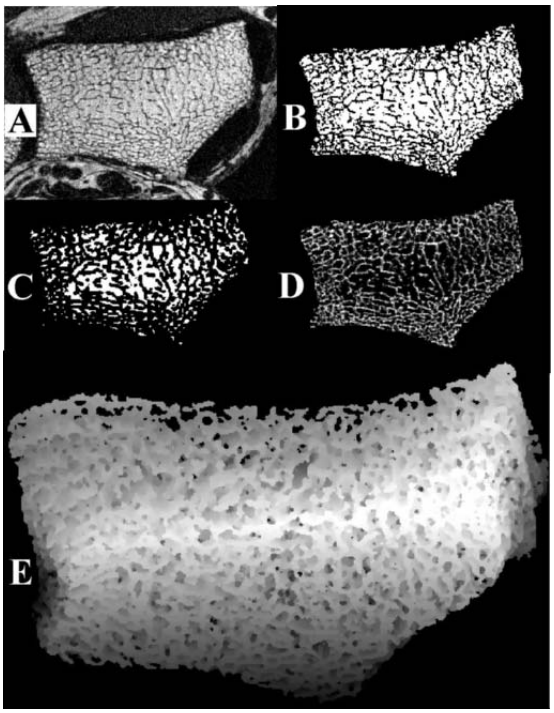


Fig 1: Fast BVF mapping.

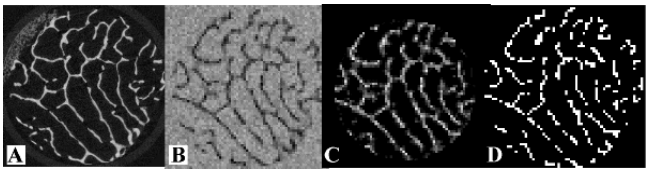


Fig 2: Evaluation with micro-CT.

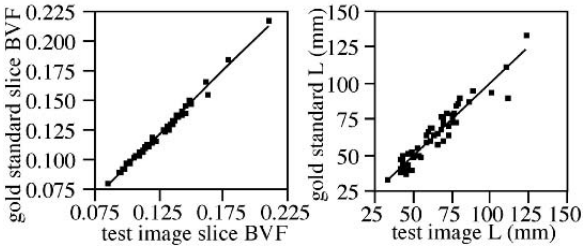


Fig. 3: Quantitative evaluation.

References

1. C. L. Gordon et al. Med. Phys. 24, 585 (1997). **2**. S. Majumdar et al. J Bone Miner Res 12, 111 (1997). **3**. T. M. Link et al. J Bone Miner Res 13, 1175 (1998). **4**. F. W. Wehrli et al. Radiology 206, 347 (1998). **5**. S. N. Hwang and F. W. Wehrli. Int. J. Imag. Sci. Tech. 10, 186 (1999). **6**. J. Ma et al. Magn. Reson. Med. 35, 903 (1996). **7**. H. K. Song and F. W. Wehrli. Magn. Reson. Med. 41, 947 (1999). **8**. H. Gudbjartsson and S. Patz. Magn. Reson. Med. 34, 910 (1995).